Belle-CONF-1402
For the Tau-2014 conference

arXiv:1409.4969v1 [hep-ex] 17 Sep 2014

Study of Michel parameters in leptonic τ decays at Belle

A. Abdesselam,[77] I. Adachi,[18,14] K. Adamczyk,[56] H. Aihara,[83] S. Al Said,[77,36] K. Arinstein,[4] Y. Arita,[49] D. M. Asner,[62] T. Aso,[88] V. Aulchenko,[4] T. Aushev,[31] R. Ayad,[77] T. Aziz,[78] S. Bahinipati,[22] A. M. Bakich,[76] A. Bala,[63] Y. Ban,[64] V. Bansal,[62] E. Barberio,[46] M. Barrett,[17] W. Bartel,[9] A. Bay,[41] I. Bedny,[4] P. Behera,[24] M. Belhorn,[8] K. Belous,[28] V. Bhardwaj,[52] B. Bhuyan,[23] M. Bischofberger,[52] S. Blyth,[54] A. Bobrov,[4] A. Bondar,[4] G. Bonvicini,[90] C. Bookwalter,[62] C. Boulahouache,[77] A. Bozek,[56] M. Bračko,[44,32] J. Brodzicka,[56] O. Brovchenko,[34] T. E. Browder,[17] D. Červenkov,[5] M.-C. Chang,[10] P. Chang,[55] Y. Chao,[55] V. Chekelian,[45] A. Chen,[53] K.-F. Chen,[55] P. Chen,[55] B. G. Cheon,[16] K. Chilikin,[31] R. Chistov,[31] K. Cho,[37] V. Chobanova,[45] S.-K. Choi,[15] Y. Choi,[75] D. Cinabro,[90] J. Crnkovic,[21] J. Dalseno,[45,79] M. Danilov,[31,47] J. Dingfelder,[3] Z. Doležal,[5] Z. Drásal,[5] A. Drutskoy,[31,47] D. Dutta,[23] K. Dutta,[23] S. Eidelman,[4] D. Epifanov,[83] S. Esen,[8] H. Farhat,[90] J. E. Fast,[62] M. Feindt,[34] T. Ferber,[9] A. Frey,[13] O. Frost,[9] M. Fujikawa,[52] V. Gaur,[78] N. Gabyshev,[4] S. Ganguly,[90] A. Garmash,[4] R. Gillard,[90] F. Giordano,[21] R. Glattauer,[27] Y. M. Goh,[16] B. Golob,[42,32] M. Grosse Perdekamp,[21,69] O. Grzymkowska,[56] H. Guo,[71] J. Haba,[18,14] P. Hamer,[13] Y. L. Han,[26] K. Hara,[18] T. Hara,[18,14] Y. Hasegawa,[73] J. Hasenbusch,[3] K. Hayasaka,[50] H. Hayashii,[52] X. H. He,[64] M. Heck,[34] D. Heffernan,[61] M. Heider,[34] T. Higuchi,[35] S. Himori,[82] T. Horiguchi,[82] Y. Horii,[50] Y. Hoshi,[81] K. Hoshina,[86] W.-S. Hou,[55] Y. B. Hsiung,[55] M. Huschle,[34] H. J. Hyun,[40] Y. Igarashi,[18] T. Iijima,[50,49] M. Imamura,[49] K. Inami,[49] A. Ishikawa,[82] K. Itagaki,[82] R. Itoh,[18,14] M. Iwabuchi,[92] M. Iwasaki,[83] Y. Iwasaki,[18] T. Iwashita,[35] S. Iwata,[85] I. Jaegle,[17] M. Jones,[17] K. K. Joo,[7] T. Julius,[46] D. H. Kah,[40] H. Kakuno,[85] J. H. Kang,[92] P. Kapusta,[56] S. U. Kataoka,[51] N. Katayama,[18] E. Kato,[82] Y. Kato,[49] P. Katrenko,[31] H. Kawai,[6] T. Kawasaki,[58] H. Kichimi,[18] C. Kiesling,[45] B. H. Kim,[72] D. Y. Kim,[74] H. J. Kim,[40] H. O. Kim,[40] J. B. Kim,[38] J. H. Kim,[37] K. T. Kim,[38] M. J. Kim,[40] S. K. Kim,[72] Y. J. Kim,[37] K. Kinoshita,[8] C. Kleinwort,[9] J. Klucar,[32] B. R. Ko,[38] N. Kobayashi,[84] S. Koblitz,[45] P. Kodyš,[5] Y. Koga,[49] S. Korpar,[44,32] R. T. Kouzes,[62] P. Križan,[42,32] P. Krokovny,[4] B. Kronenbitter,[34] T. Kuhr,[34] R. Kumar,[66] T. Kumita,[85] E. Kurihara,[6] Y. Kuroki,[61] A. Kuzmin,[4] P. Kvasnička,[5] Y.-J. Kwon,[92] Y.-T. Lai,[55] J. S. Lange,[11] S.-H. Lee,[38] M. Leitgab,[21,69] R. Leitner,[5] J. Li,[72] X. Li,[72] Y. Li,[89] L. Li Gioi,[45] J. Libby,[24] A. Limosani,[46] C. Liu,[71] Y. Liu,[8] Z. Q. Liu,[26] D. Liventsev,[18] R. Louvot,[41] P. Lukin,[4] J. MacNaughton,[18] D. Matvienko,[4] A. Matyja,[56] S. McOnie,[76] Y. Mikami,[82] K. Miyabayashi,[52] Y. Miyachi,[91] H. Miyake,[18,14] H. Miyata,[58] Y. Miyazaki,[49] R. Mizuk,[31,47] G. B. Mohanty,[78] D. Mohapatra,[62] A. Moll,[45,79] T. Mori,[49] H.-G. Moser,[45] T. Müller,[34] N. Muramatsu,[67] R. Mussa,[30] T. Nagamine,[82] Y. Nagasaka,[19] Y. Nakahama,[83] I. Nakamura,[18,14] K. Nakamura,[18] E. Nakano,[60] H. Nakano,[82] T. Nakano,[68] M. Nakao,[18] H. Nakayama,[18] H. Nakazawa,[53] T. Nanut,[32] Z. Natkaniec,[56] M. Nayak,[24] E. Nedelkovska,[45] K. Negishi,[82] K. Neichi,[81] C. Ng,[83] C. Niebuhr,[9] M. Niiyama,[39] N. K. Nisar,[78]

S. Nishida,[18,14] K. Nishimura,[17] O. Nitoh,[86] T. Nozaki,[18] A. Ogawa,[69] S. Ogawa,[80] T. Ohshima,[49] S. Okuno,[33] S. L. Olsen,[72] Y. Ono,[82] Y. Onuki,[83] W. Ostrowicz,[56] C. Oswald,[3] H. Ozaki,[18,14] P. Pakhlov,[31,47] G. Pakhlova,[31] H. Palka,[56] E. Panzenböck,[13,52] C.-S. Park,[92] C. W. Park,[75] H. Park,[40] H. K. Park,[40] K. S. Park,[75] L. S. Peak,[76] T. K. Pedlar,[43] T. Peng,[71] L. Pesantez,[3] R. Pestotnik,[32] M. Peters,[17] M. Petrič,[32] L. E. Piilonen,[89] A. Poluektov,[4] M. Prim,[34] K. Prothmann,[45,79] B. Reisert,[45] E. Ribežl,[32] M. Ritter,[45] M. Röhrken,[34] J. Rorie,[17] A. Rostomyan,[9] M. Rozanska,[56] S. Ryu,[72] H. Sahoo,[17] T. Saito,[82] K. Sakai,[18] Y. Sakai,[18,14] S. Sandilya,[78] D. Santel,[8] L. Santelj,[32] T. Sanuki,[82] N. Sasao,[39] Y. Sato,[82] V. Savinov,[65] O. Schneider,[41] G. Schnell,[1,20] P. Schönmeier,[82] M. Schram,[62] C. Schwanda,[27] A. J. Schwartz,[8] B. Schwenker,[13] R. Seidl,[69] A. Sekiya,[52] D. Semmler,[11] K. Senyo,[91] O. Seon,[49] M. E. Sevior,[46] L. Shang,[26] M. Shapkin,[28] V. Shebalin,[4] C. P. Shen,[2] T.-A. Shibata,[84] H. Shibuya,[80] S. Shinomiya,[61] J.-G. Shiu,[55] B. Shwartz,[4] A. Sibidanov,[76] F. Simon,[45,79] J. B. Singh,[63] R. Sinha,[29] P. Smerkol,[32] Y.-S. Sohn,[92] A. Sokolov,[28] Y. Soloviev,[9] E. Solovieva,[31] S. Stanič,[59] M. Starič,[32] M. Steder,[9] J. Stypula,[56] S. Sugihara,[83] A. Sugiyama,[70] M. Sumihama,[12] K. Sumisawa,[18,14] T. Sumiyoshi,[85] K. Suzuki,[49] S. Suzuki,[70] S. Y. Suzuki,[18] Z. Suzuki,[82] H. Takeichi,[49] U. Tamponi,[30,87] M. Tanaka,[18,14] S. Tanaka,[18,14] K. Tanida,[72] N. Taniguchi,[18] G. Tatishvili,[62] G. N. Taylor,[46] Y. Teramoto,[60] F. Thorne,[27] I. Tikhomirov,[31] K. Trabelsi,[18,14] Y. F. Tse,[46] T. Tsuboyama,[18,14] M. Uchida,[84] T. Uchida,[18] Y. Uchida,[14] S. Uehara,[18,14] K. Ueno,[55] T. Uglov,[31,48] Y. Unno,[16] S. Uno,[18,14] P. Urquijo,[3] Y. Ushiroda,[18,14] Y. Usov,[4] S. E. Vahsen,[17] C. Van Hulse,[1] P. Vanhoefer,[45] G. Varner,[17] K. E. Varvell,[76] K. Vervink,[41] A. Vinokurova,[4] V. Vorobyev,[4] A. Vossen,[25] M. N. Wagner,[11] C. H. Wang,[54] J. Wang,[64] M.-Z. Wang,[55] P. Wang,[26] X. L. Wang,[89] M. Watanabe,[58] Y. Watanabe,[33] R. Wedd,[46] S. Wehle,[9] E. White,[8] J. Wiechczynski,[56] K. M. Williams,[89] E. Won,[38] B. D. Yabsley,[76] S. Yamada,[18] H. Yamamoto,[82] J. Yamaoka,[62] Y. Yamashita,[57] M. Yamauchi,[18,14] S. Yashchenko,[9] Y. Yook,[92] C. Z. Yuan,[26] Y. Yusa,[58] D. Zander,[34] C. C. Zhang,[26] L. M. Zhang,[71] Z. P. Zhang,[71] L. Zhao,[71] V. Zhilich,[4] P. Zhou,[90] V. Zhulanov,[4] T. Zivko,[32] A. Zupanc,[32] N. Zwahlen,[41] and O. Zyukova[4]

(The Belle Collaboration)

[1]*University of the Basque Country UPV/EHU, 48080 Bilbao*
[2]*Beihang University, Beijing 100191*
[3]*University of Bonn, 53115 Bonn*
[4]*Budker Institute of Nuclear Physics SB RAS and Novosibirsk State University, Novosibirsk 630090*
[5]*Faculty of Mathematics and Physics, Charles University, 121 16 Prague*
[6]*Chiba University, Chiba 263-8522*
[7]*Chonnam National University, Kwangju 660-701*
[8]*University of Cincinnati, Cincinnati, Ohio 45221*
[9]*Deutsches Elektronen–Synchrotron, 22607 Hamburg*
[10]*Department of Physics, Fu Jen Catholic University, Taipei 24205*
[11]*Justus-Liebig-Universität Gießen, 35392 Gießen*
[12]*Gifu University, Gifu 501-1193*
[13]*II. Physikalisches Institut, Georg-August-Universität Göttingen, 37073 Göttingen*
[14]*The Graduate University for Advanced Studies, Hayama 240-0193*

[15]*Gyeongsang National University, Chinju 660-701*
[16]*Hanyang University, Seoul 133-791*
[17]*University of Hawaii, Honolulu, Hawaii 96822*
[18]*High Energy Accelerator Research Organization (KEK), Tsukuba 305-0801*
[19]*Hiroshima Institute of Technology, Hiroshima 731-5193*
[20]*IKERBASQUE, Basque Foundation for Science, 48011 Bilbao*
[21]*University of Illinois at Urbana-Champaign, Urbana, Illinois 61801*
[22]*Indian Institute of Technology Bhubaneswar, Satya Nagar 751007*
[23]*Indian Institute of Technology Guwahati, Assam 781039*
[24]*Indian Institute of Technology Madras, Chennai 600036*
[25]*Indiana University, Bloomington, Indiana 47408*
[26]*Institute of High Energy Physics,*
Chinese Academy of Sciences, Beijing 100049
[27]*Institute of High Energy Physics, Vienna 1050*
[28]*Institute for High Energy Physics, Protvino 142281*
[29]*Institute of Mathematical Sciences, Chennai 600113*
[30]*INFN - Sezione di Torino, 10125 Torino*
[31]*Institute for Theoretical and Experimental Physics, Moscow 117218*
[32]*J. Stefan Institute, 1000 Ljubljana*
[33]*Kanagawa University, Yokohama 221-8686*
[34]*Institut für Experimentelle Kernphysik,*
Karlsruher Institut für Technologie, 76131 Karlsruhe
[35]*Kavli Institute for the Physics and Mathematics of the Universe (WPI),*
University of Tokyo, Kashiwa 277-8583
[36]*Department of Physics, Faculty of Science,*
King Abdulaziz University, Jeddah 21589
[37]*Korea Institute of Science and Technology Information, Daejeon 305-806*
[38]*Korea University, Seoul 136-713*
[39]*Kyoto University, Kyoto 606-8502*
[40]*Kyungpook National University, Daegu 702-701*
[41]*École Polytechnique Fédérale de Lausanne (EPFL), Lausanne 1015*
[42]*Faculty of Mathematics and Physics,*
University of Ljubljana, 1000 Ljubljana
[43]*Luther College, Decorah, Iowa 52101*
[44]*University of Maribor, 2000 Maribor*
[45]*Max-Planck-Institut für Physik, 80805 München*
[46]*School of Physics, University of Melbourne, Victoria 3010*
[47]*Moscow Physical Engineering Institute, Moscow 115409*
[48]*Moscow Institute of Physics and Technology, Moscow Region 141700*
[49]*Graduate School of Science, Nagoya University, Nagoya 464-8602*
[50]*Kobayashi-Maskawa Institute, Nagoya University, Nagoya 464-8602*
[51]*Nara University of Education, Nara 630-8528*
[52]*Nara Women's University, Nara 630-8506*
[53]*National Central University, Chung-li 32054*
[54]*National United University, Miao Li 36003*
[55]*Department of Physics, National Taiwan University, Taipei 10617*
[56]*H. Niewodniczanski Institute of Nuclear Physics, Krakow 31-342*

[57]Nippon Dental University, Niigata 951-8580
[58]Niigata University, Niigata 950-2181
[59]University of Nova Gorica, 5000 Nova Gorica
[60]Osaka City University, Osaka 558-8585
[61]Osaka University, Osaka 565-0871
[62]Pacific Northwest National Laboratory, Richland, Washington 99352
[63]Panjab University, Chandigarh 160014
[64]Peking University, Beijing 100871
[65]University of Pittsburgh, Pittsburgh, Pennsylvania 15260
[66]Punjab Agricultural University, Ludhiana 141004
[67]Research Center for Electron Photon Science,
Tohoku University, Sendai 980-8578
[68]Research Center for Nuclear Physics, Osaka University, Osaka 567-0047
[69]RIKEN BNL Research Center, Upton, New York 11973
[70]Saga University, Saga 840-8502
[71]University of Science and Technology of China, Hefei 230026
[72]Seoul National University, Seoul 151-742
[73]Shinshu University, Nagano 390-8621
[74]Soongsil University, Seoul 156-743
[75]Sungkyunkwan University, Suwon 440-746
[76]School of Physics, University of Sydney, NSW 2006
[77]Department of Physics, Faculty of Science, University of Tabuk, Tabuk 71451
[78]Tata Institute of Fundamental Research, Mumbai 400005
[79]Excellence Cluster Universe, Technische Universität München, 85748 Garching
[80]Toho University, Funabashi 274-8510
[81]Tohoku Gakuin University, Tagajo 985-8537
[82]Tohoku University, Sendai 980-8578
[83]Department of Physics, University of Tokyo, Tokyo 113-0033
[84]Tokyo Institute of Technology, Tokyo 152-8550
[85]Tokyo Metropolitan University, Tokyo 192-0397
[86]Tokyo University of Agriculture and Technology, Tokyo 184-8588
[87]University of Torino, 10124 Torino
[88]Toyama National College of Maritime Technology, Toyama 933-0293
[89]CNP, Virginia Polytechnic Institute and State University, Blacksburg, Virginia 24061
[90]Wayne State University, Detroit, Michigan 48202
[91]Yamagata University, Yamagata 990-8560
[92]Yonsei University, Seoul 120-749

Abstract

We present a study of Michel parameters in leptonic τ decays using experimental information collected at the Belle detector. Michel parameters are extracted in the unbinned maximum likelihood fit of the $(\tau^{\mp} \to \ell^{\mp}\nu\nu,\ \tau^{\pm} \to \pi^{\pm}\pi^{0}\nu)$ events in the full nine-dimensional phase space. We exploit the spin-spin correlation of tau leptons to extract $\xi_\rho\xi$ and $\xi_\rho\xi\delta$ in addition to the ρ and η parameters.

PACS numbers: 13.35.Dx, 13.66.De, 13.66.Jn, 14.60.Fg

INTRODUCTION

In the Standard Model (SM), the charged weak interaction is described by the exchange of a $W^{\pm}$ boson with a pure vector coupling to only left-chirality fermions. Thus, in the low-energy four-fermion framework, the Lorentz structure of the matrix element is predicted to be of the "V-A⊗V-A" type. Deviations from this behavior would indicate new physics and might be caused either by changes in the W-boson couplings or through interactions mediated by new gauge bosons. Leptonic decays such as $\tau^- \to \ell^- \bar{\nu}_\ell \nu_\tau$ ($\ell = e, \mu$) (unless specified otherwise, charge-conjugated decays are implied throughout the paper) are the only ones in which the electroweak couplings can be probed without disturbance from the strong interaction. This makes them an ideal system to study the Lorentz structure of the charged weak current.

The most general, Lorentz invariant, derivative-free and lepton-number-conserving four-lepton point interaction matrix element for this decay can be written as [1]:

$$\mathcal{M} = \frac{4G}{\sqrt{2}} \sum_{\substack{N=S,V,T \\ i,j=L,R}} g_{ij}^N \Big[\bar{u}_i(l^-) \Gamma^N v_n(\bar{\nu}_l) \Big] \Big[\bar{u}_m(\nu_\tau) \Gamma_N u_j(\tau^-) \Big], \tag{1}$$

$$\Gamma^S = 1,\ \Gamma^V = \gamma^\mu,\ \Gamma^T = \frac{1}{\sqrt{2}} \sigma^{\mu\nu} = \frac{i}{2\sqrt{2}} (\gamma^\mu \gamma^\nu - \gamma^\nu \gamma^\mu) \tag{2}$$

The Γ_N matrices define the properties of the two currents under a Lorentz transformation with $N = S, V, T$ for scalar, vector and tensor interactions, respectively. The indices i and j label the right- or left-handedness (R, L) of the charged leptons. For a given i, j and N, the handedness of the neutrinos (n, m) is fixed. Ten non-trivial terms are characterized by ten complex coupling constants g_{ij}^N; those with g_{RR}^T and g_{LL}^T are identically zero. In the SM, the only non-zero coupling constant is $g_{LL}^V = 1$. As the couplings can be complex, with arbitrary overall phase, there are 19 independent parameters. The total strength of the weak interaction (charged weak current sector) is determined by the Fermi constant G, hence, the g_{ij}^N are normalized as:

$$3\Big(|g_{LR}^T|^2 + |g_{RL}^T|^2 \Big) + \Big(|g_{LL}^V|^2 + |g_{LR}^V|^2 + |g_{RL}^V|^2 + |g_{RR}^V|^2 \Big) + \\ + \frac{1}{4} \Big(|g_{LL}^S|^2 + |g_{LR}^S|^2 + |g_{RL}^S|^2 + |g_{RR}^S|^2 \Big) \equiv 1 \tag{3}$$

This constrains the coupling constants to be $|g_{ij}^S| \leq 2$, $|g_{ij}^V| \leq 1$ and $|g_{ij}^T| \leq 1/\sqrt{3}$.

In the case where neutrinos are not detected and the spin of the outgoing charged lepton is not determined, only four Michel parameters (MP) ρ, η, ξ and δ are experimentally accessible. They are bilinear combinations of the g_{ij}^N coupling constants [2]:

$$\rho = \frac{3}{4} - \frac{3}{4} \Big(|g_{LR}^V|^2 + |g_{RL}^V|^2 + 2|g_{LR}^T|^2 + 2|g_{RL}^T|^2 + \Re\big(g_{LR}^S g_{LR}^{T*} + g_{RL}^S g_{RL}^{T*} \big) \Big) \tag{4}$$

$$\eta = \frac{1}{2} \Re \Big(6 g_{RL}^V g_{LR}^{T*} + 6 g_{LR}^V g_{RL}^{T*} + g_{RR}^S g_{LL}^{V*} + g_{RL}^S g_{LR}^{V*} + g_{LR}^S g_{RL}^{V*} + g_{LL}^S g_{RR}^{V*} \Big) \tag{5}$$

$$\xi = 4\Re(g_{LR}^S g_{LR}^{T*}) - 4\Re(g_{RL}^S g_{RL}^{T*}) + |g_{LL}^V|^2 + 3|g_{LR}^V|^2 - 3|g_{RL}^V|^2 - |g_{RR}^V|^2$$

$$+ 5|g^T_{LR}|^2 - 5|g^T_{RL}|^2 + \frac{1}{4}|g^S_{LL}|^2 - \frac{1}{4}|g^S_{LR}|^2 + \frac{1}{4}|g^S_{RL}|^2 - \frac{1}{4}|g^S_{RR}|^2 \quad (6)$$

$$\xi\delta = \frac{3}{16}|g^S_{LL}|^2 - \frac{3}{16}|g^S_{LR}|^2 + \frac{3}{16}|g^S_{RL}|^2 - \frac{3}{16}|g^S_{RR}|^2 - \frac{3}{4}|g^T_{LR}|^2 + \frac{3}{4}|g^T_{RL}|^2$$
$$+ \frac{3}{4}|g^V_{LL}|^2 - \frac{3}{4}|g^V_{RR}|^2 + \frac{3}{4}\Re\big(g^S_{LR}g^{T*}_{LR}\big) - \frac{3}{4}\Re\big(g^S_{RL}g^{T*}_{RL}\big) \quad (7)$$

and appear in the predicted energy spectrum of the charged lepton.

In the τ rest frame, neglecting radiative corrections, this spectrum is given by [3]:

$$\frac{d\Gamma(\tau^\mp)}{d\Omega dx} = \frac{4G^2M_\tau E^4_{\max}}{(2\pi)^4}\sqrt{x^2-x_0^2}\bigg(x(1-x) + \frac{2}{9}\rho(4x^2-3x-x_0^2) + \eta x_0(1-x)$$
$$\mp\frac{1}{3}P_\tau\cos\theta_\ell\xi\sqrt{x^2-x_0^2}\bigg[1-x+\frac{2}{3}\delta\big(4x-4+\sqrt{1-x_0^2}\big)\bigg]\bigg),$$
$$x = \frac{E_\ell}{E_{max}},\ E_{max} = \frac{M_\tau}{2}(1+\frac{m_\ell^2}{M_\tau^2}),\ x_0 = \frac{m_\ell}{E_{max}}, \quad (8)$$

where P_τ is τ polarization, and θ_ℓ is the angle between the τ spin and the lepton momentum. In the SM, the "V-A" charged weak current is characterized by $\rho = 3/4$, $\eta = 0$, $\xi = 1$ and $\delta = 3/4$.

METHOD

Measurement of ξ and δ requires knowledge of the τ spin direction. In experiments at e^+e^- colliders with unpolarized $e^\pm$ beams, the average polarization of a single τ is zero. However, spin-spin correlations between the τ^+ and τ^- produced in the reaction $e^+e^- \to \tau^+\tau^-$ can be exploited [4]. The main idea of our method is to consider events where both taus decay to selected final states. One (signal) tau decays leptonically ($\tau^- \to \ell^-\nu_\tau\bar\nu_\ell$, $\ell = e,\ \mu$) while the opposite tau, which decays via $\tau^+ \to \pi^+\pi^0\bar\nu_\tau$, serves as a spin analyser. We choose the $\tau^+ \to \pi^+\pi^0\bar\nu_\tau$ decay mode because it has the largest branching fraction as well as properly studied dynamics [5]. To write the total differential cross section for ($\tau^- \to \ell^-\nu_\tau\bar\nu_\ell$, $\tau^+ \to \pi^+\pi^0\bar\nu_\tau$) (or, briefly, $\ell-\rho$) events, we follow the approach developed in Refs. [6–8]. The differential cross section of the $e^+e^- \to \tau^+(\vec\zeta^{*+})\tau^-(\vec\zeta^{*-})$ reaction in the center-of-mass system (c.m.s.) is given by their formula [4]:

$$\frac{d\sigma(\vec\zeta^{*-},\vec\zeta^{*+})}{d\Omega} = \frac{\alpha^2}{64E_\tau^2}\beta_\tau(D_0 + D_{ij}\zeta_i^{*-}\zeta_j^{*+}), \quad (9)$$

where $D_0 = 1+\cos^2\theta + \frac{1}{\gamma_\tau^2}\sin^2\theta$, D_{ij} is the spin-spin correlation tensor, and $\vec\zeta^{*\mp}$ is the polarisation vector of the $\tau^\mp$ in the $\tau^\mp$ rest frame (unit vector along the $\tau^\mp$ spin direction). The asterisk denotes a parameter measured in the associated τ rest frame. The differential decay width of the signal is written in the form (with the total normalization constant κ_ℓ that is unimportant in this context):

$$\frac{d\Gamma(\tau^\mp(\vec\zeta^{*\mp}) \to \ell^\mp\nu\nu)}{dx^*d\Omega_\ell^*} = \kappa_\ell(A(x^*) \mp \xi\vec n_\ell^*\vec\zeta^{*\mp}B(x^*)),$$

$$A(x^*) = A_0(x^*) + \rho A_1(x^*) + \eta A_2(x^*),\ B(x^*) = B_1(x^*) + \delta B_2(x^*), \tag{10}$$

where the form factors $A_0,\ A_1,\ A_2,\ B_1$ and B_2 can be extracted from Eq. 8. The $\tau^{\pm}(\vec{\zeta'}^*) \to \rho^{\pm}(K^*)\nu(q^*) \to \pi^{\pm}(p_1^*)\pi^0(p_2^*)\nu(q^*)$ decay width reads (with the total normalization constant κ_ρ):

$$\frac{d\Gamma(\tau^{\pm} \to \pi^{\pm}\pi^0\nu)}{dm^2_{\pi\pi}d\Omega^*_\rho d\tilde{\Omega}_\pi} = \kappa_\rho(A' \mp \vec{B'}\vec{\zeta'}^*)W(m^2_{\pi\pi}), \tag{11}$$

$$A' = 2(q,Q)Q_0^* - Q^2 q_0^*,\ \vec{B'} = Q^2\vec{K}^* + 2(q,Q)\vec{Q}^*,\ Q^* = p_1^* - p_2^*,\ K^* = p_1^* + p_2^*,$$

$$W(m^2_{\pi\pi}) = |F_\pi(m^2_{\pi\pi})|^2 \frac{p^*_\rho(m^2_{\pi\pi})\tilde{p}_\pi(m^2_{\pi\pi})}{M_\tau m_{\pi\pi}},\ m^2_{\pi\pi} = K^{*2},\ p^*_\rho = \frac{M_\tau}{2}\left(1 - \frac{m^2_{\pi\pi}}{M^2_\tau}\right),$$

$$\tilde{p}_\pi = \frac{\sqrt{(m^2_{\pi\pi} - (m_\pi + m_{\pi^0})^2)(m^2_{\pi\pi} - (m_\pi - m_{\pi^0})^2)}}{2m_{\pi\pi}}, \tag{12}$$

where p^*_ρ and Ω^*_ρ are the momentum and solid angle of the ρ meson in the τ rest frame; $\tilde{p}_\pi$ and $\tilde{\Omega}_\pi$ are the momentum and solid angle of the charged pion in the ρ rest frame; and $F_\pi(m^2_{\pi\pi})$ is the pion form factor taken from Ref. [5]. The total differential cross section for $\ell - \rho$ events is:

$$\frac{d\sigma(\ell^{\mp}, \rho^{\pm})}{dE^*_\ell d\Omega^*_\ell d\Omega^*_\rho dm^2_{\pi\pi} d\tilde{\Omega}_\pi d\Omega_\tau} = \kappa_\ell\kappa_\rho \frac{\alpha^2\beta_\tau}{64E^2_\tau}\big(D_0 A'A + \xi_\rho\xi D_{ij}n^*_{\ell i}B'_j B\big)W(m^2_{\pi\pi}) \tag{13}$$

Experimentally, we measure particle parameters in the c.m.s.; hence, the visible differential cross section is given by [7]:

$$\frac{d\sigma(\ell^{\mp}, \rho^{\pm})}{dp_\ell d\Omega_\ell dp_\rho d\Omega_\rho dm^2_{\pi\pi} d\tilde{\Omega}_\pi} = \int_{\Phi_1}^{\Phi_2} \frac{d\sigma(\ell^{\mp}, \rho^{\pm})}{dE^*_\ell d\Omega^*_\ell d\Omega^*_\rho dm^2_{\pi\pi} d\tilde{\Omega}_\pi d\Omega_\tau} \left|\frac{\partial(E^*_\ell, \Omega^*_\ell, \Omega^*_\rho, \Omega_\tau)}{\partial(p_\ell, \Omega_\ell, p_\rho, \Omega_\rho, \Phi_\tau)}\right| d\Phi_\tau, \tag{14}$$

where the integration is performed over the unknown τ direction, which is constrained by the (Φ_1, Φ_2) arc. Both Φ_1 and Φ_2 are calculated using parameters measured in the experiment. The differential cross section is used to construct the probability density function (p.d.f.) for the measurement vector $\vec{z} = (p_\ell,\ \cos\theta_\ell,\ \phi_\ell,\ p_\rho,\ \cos\theta_\rho,\ \phi_\rho,\ m_{\pi\pi},\ \cos\tilde{\theta}_\pi,\ \tilde{\phi}_\pi)$:

$$\mathcal{P}(\vec{z}) = \frac{\mathcal{F}(\vec{z})}{\int \mathcal{F}(\vec{z})d\vec{z}},\ \mathcal{F}(\vec{z}) = \frac{d\sigma(\ell^{\mp}, \rho^{\pm})}{dp_\ell d\Omega_\ell dp_\rho d\Omega_\rho dm^2_{\pi\pi} d\tilde{\Omega}_\pi} = \mathcal{F}_0 + \mathcal{F}_1\rho + \mathcal{F}_2\eta + \mathcal{F}_3\xi_\rho\xi + \mathcal{F}_4\xi_\rho\xi\delta,$$

$$\mathcal{N} = \int \mathcal{F}(\vec{z})d\vec{z} = \mathcal{N}_0 + \mathcal{N}_1\rho + \mathcal{N}_2\eta + \mathcal{N}_3\xi_\rho\xi + \mathcal{N}_4\xi_\rho\xi\delta,\ \mathcal{N}_i = \int \mathcal{F}_i(\vec{z})d\vec{z},\ i = 0...4,$$

$$\mathcal{P}(\vec{z}) = \frac{\mathcal{F}_0(\vec{z}) + \mathcal{F}_1(\vec{z})\rho + \mathcal{F}_2(\vec{z})\eta + \mathcal{F}_3(\vec{z})\xi_\rho\xi + \mathcal{F}_4(\vec{z})\xi_\rho\xi\delta}{\mathcal{N}_0 + \mathcal{N}_1\rho + \mathcal{N}_2\eta + \mathcal{N}_3\xi_\rho\xi + \mathcal{N}_4\xi_\rho\xi\delta}, \tag{15}$$

where the form factors $\mathcal{F}_i$ are calculated for each event and the five normalisation constants $\mathcal{N}_i$ are evaluated using a Monte Carlo (MC) simulated sample. There are several corrections that must be incorporated in the procedure to take into account the real experimental situation. Physics corrections include electroweak higher-order corrections to the $e^+e^- \to \tau^+\tau^-$ cross section [9–15], the effect of the radiative leptonic decay $\tau^- \to \ell^-\bar{\nu}_\ell\nu_\tau\gamma$ [16–18], and the effect of the radiative hadronic decay $\tau^- \to \pi^-\pi^0\nu_\tau\gamma$ [19, 20]. Apparatus corrections

include the effect of the finite detection efficiency and resolution, the effect of the external bremsstrahlung for $e-\rho$ events, and the $e^{\pm}$ beam energy spread.

The method described is used for a precise measurement of Michel parameters in $\ell-\rho$ events. This analysis is based on a 485 fb^{-1} data sample that contains 446 $\times 10^6$ $\tau^+\tau^-$ pairs, collected with the Belle detector at the KEKB energy-asymmetric e^+e^- (3.5 on 8 GeV) collider [21] operating at the $\Upsilon(4S)$ resonance.

THE BELLE DETECTOR

The Belle detector is a large-solid-angle magnetic spectrometer that consists of a silicon vertex detector (SVD), a 50-layer central drift chamber (CDC), an array of aerogel threshold Cherenkov counters (ACC), a barrel-like arrangement of time-of-flight scintillation counters (TOF), and an electromagnetic calorimeter (ECL) comprised of CsI(Tl) crystals located inside a superconducting solenoid coil that provides a 1.5 T magnetic field. An iron flux-return located outside the coil is instrumented to detect K_L^0 mesons and to identify muons (KLM). Two inner detector configurations are used in this analysis. A beampipe with a radius of 2.0 cm and a 3-layer silicon vertex detector are used for the first sample of 124×10^6 $\tau^+\tau^-$ pairs, while a 1.5 cm beampipe, a 4-layer silicon detector and a small-cell inner drift chamber are used to record the remaining 322×10^6 $\tau^+\tau^-$ pairs [22]. The detector is described in detail elsewhere [23].

SELECTION OF $\ell-\rho$ EVENTS, BACKGROUND

This analysis is based on events with one τ decaying to leptons $\tau^- \to \ell^-\bar{\nu}_\ell\nu_\tau$ and the other decaying via the hadronic channel $\tau^+ \to \pi^+\pi^0\bar{\nu}_\tau$.

The selection process, which is designed to suppress background while retaining a high efficiency for the decays under study, proceeds in two stages.

1) The first-stage criteria suppress beam background to a negligible level and reject most of the background from other physical processes:

- There should be exactly two tracks extrapolated to the interaction point within ± 0.5 cm in the transverse direction and ± 2.5 cm along the beam and having a transverse momentum in the c.m.s. $|\vec{P}|_\perp^{\rm CM} > 0.1$ GeV/c and a net charge of zero.
- The sum of the track absolute momenta in the c.m.s. must satisfy $P^{\rm CM} < 9$ GeV/c.
- The maximum value of the transverse momentum for all tracks in the laboratory frame should satisfy $|\vec{P}|_\perp^{\rm LAB} > 0.5$ GeV/c.
- The maximum opening angle ψ between tracks should exceed 20°.
- The number of photons N_γ with c.m.s. energy $E_\gamma^{\rm CM} > 80$ MeV should be five or fewer.
- The total ECL energy deposition in the laboratory frame should satisfy $\sum_{i=1}^{N_{\rm clusters}} E_i^{\rm LAB}({\rm ECL}) < 9$ GeV.
- The total energy of additional photons in the laboratory frame should be $\sum E_{{\rm rest}\gamma}^{\rm LAB} < 0.2$ GeV.

- The missing mass should lie in the range 1 GeV/$c^2 \leq M_{\rm miss} \leq 7$ GeV/c^2.
- The polar angle of the missing momentum in the c.m.s. should satisfy $30^\circ \leq \theta^{\rm CM}_{\rm miss} \leq 150^\circ$.

The last two criteria are especially effective in suppressing background from radiative Bhabha, $\mu^+\mu^-$ and two-photon processes.

2) In the second stage, the $\ell^\mp - \rho^\pm$ ($\ell = e, \mu$, $\rho^\pm \to \pi^\pm\pi^0$) samples are selected from the remaining events.

To select electrons, a likelihood ratio cut $\mathcal{P}_e = \mathcal{L}_e/(\mathcal{L}_e + \mathcal{L}_x) > 0.8$ is applied, where the electron likelihood function $\mathcal{L}_e$ and the non-electron function $\mathcal{L}_x$ include information on the specific ionization (dE/dx) measurement by the CDC, the ratio of the cluster energy in the ECL to the track momentum measured in the CDC, the transverse ECL shower shape and the light yield in the ACC [24]. The efficiency of this cut for electrons is 93.1%.

To select muons, the likelihood ratio cut $\mathcal{P}_\mu = \mathcal{L}_\mu/(\mathcal{L}_\mu+\mathcal{L}_\pi+\mathcal{L}_K) > 0.8$ is applied. It has an 88.0% efficiency for muons. Each of the muon($\mathcal{L}_\mu$), pion($\mathcal{L}_\pi$) and kaon($\mathcal{L}_K$) likelihood functions is evaluated from two variables: the difference between the range calculated from the momentum of the particle and the range measured by KLM and the χ^2 of the KLM hits with respect to the extrapolated track [25].

To separate pions from kaons, we determine for each track the pion ($\mathcal{L}_\pi$) and kaon ($\mathcal{L}_K$) likelihoods from the ACC response, the dE/dx measurement in the CDC and the TOF flight-time measurement, and form a likelihood ratio $\mathcal{P}_{K/\pi} = \mathcal{L}_K/(\mathcal{L}_\pi + \mathcal{L}_K)$ to separate pions and kaons. For pions, we require $\mathcal{P}_{K/\pi} < 0.6$, which provides a pion identification efficiency of about 93% while keeping the pion fake rate at the 6% level.

Finally, we select events with only one lepton $\ell^\mp$ ($\ell = e, \mu$), one charged pion $\pi^\pm$ and one π^0 candidate. A π^0 meson is reconstructed from a pair of gammas with an energy in the laboratory frame of $E^{\rm LAB}_\gamma > 80$ MeV and the $\gamma\gamma$ invariant mass in the range 115 MeV/$c^2 < M_{\gamma\gamma} <$ 150 MeV/c^2. The absolute value of the π^0 momentum in the c.m.s. must satisfy $P^{\rm CMS}_{\pi^0} > 0.3$ GeV/c. The invariant mass of the $\pi^\pm\pi^0$ system must lie in the range 0.3 GeV/$c^2 < M_{\pi^\pm\pi^0} <$ 1.8 GeV/c^2. The opening angles between a lepton and charged pion and between a lepton and π^0 should exceed 90°. To avoid the uncertainty due to the simulation of low energy fake ECL clusters, we allow additional photons in an event with the total energy in the laboratory frame of $E^{\rm LAB}_{{\rm rest}\gamma} < 0.2$ GeV.

To evaluate the background and calculate efficiencies, a Monte Carlo sample of 2.87×10^9 $\tau^+\tau^-$ pairs is produced with the KKMC/TAUOLA generators [26, 27]. The detector response is simulated by a GEANT3-based program [28].

The detection efficiencies for signal events are $\varepsilon_{\rm det}(e-\rho) = (11.53 \pm 0.01)\%$ and $\varepsilon_{\rm det}(\mu - \rho) = (12.43 \pm 0.01)\%$. It is found that the dominant background comes from other τ decays; a contribution from non-$\tau\tau$ processes is very small – less than 0.1%. The dominant background arises from ($\tau^- \to \ell^-\bar{\nu}_\ell\nu_\tau$, $\tau^+ \to \pi^+\pi^0\pi^0\bar{\nu}_\tau$) (or, briefly, $\ell - 3\pi$) events, where the second π^0 is lost. Its contribution is $\lambda_{3\pi} = 10.0\%$ for the $e-\rho$ and $\lambda_{3\pi} = 8.1\%$ for the $\mu-\rho$ events. For the $\mu-\rho$ events, an additional background at the level of $\lambda_\pi = 1.4\%$ originates from ($\tau^- \to \pi^-\nu_\tau$, $\tau^+ \to \pi^+\pi^0\bar{\nu}_\tau$) (or, briefly, $\pi-\rho$) events, where a pion is misidentified as a muon. The remaining background comes from other τ decays; its contribution is $\lambda_{\rm other} = 2.0\%$ for $e-\rho$ events and $\lambda_{\rm other} = 2.5\%$ for $\mu-\rho$ events.

The main background processes, $\ell - 3\pi$ and $\pi - \rho$, are included in the p.d.f. analytically while the remaining background is taken into account using the MC-based approach [29].

The total p.d.f. is written as:

$$\mathcal{P}(\vec{z}) = \frac{\varepsilon(\vec{z})}{\varepsilon}\Bigg((1-\lambda_{3\pi}-\lambda_{\pi}-\lambda_{\rm other})\frac{S(\vec{z})}{\int \frac{\varepsilon(\vec{z})}{\varepsilon}S(\vec{z})d\vec{z}} + \lambda_{3\pi}\frac{\tilde{B}_{3\pi}(\vec{z})}{\int \frac{\varepsilon(\vec{z})}{\varepsilon}\tilde{B}_{3\pi}(\vec{z})d\vec{z}} + \\ + \lambda_{\pi}\frac{\tilde{B}_{\pi}(\vec{z})}{\int \frac{\varepsilon(\vec{z})}{\varepsilon}\tilde{B}_{\pi}(\vec{z})d\vec{z}} + \lambda_{\rm other}\frac{B^{MC}_{\rm other}(\vec{z})}{\int \frac{\varepsilon(\vec{z})}{\varepsilon}B^{MC}_{\rm other}(\vec{z})d\vec{z}}\Bigg), \tag{16}$$

where $S(\vec{z})$, $\tilde{B}_{3\pi}(\vec{z})$ and $\tilde{B}_{\pi}(\vec{z})$ are the cross sections for the $\ell-\rho$, $\ell-3\pi$ and $\pi-\rho$ events, respectively; $\varepsilon(\vec{z})$ is the detection efficiency for signal events in the nine-dimensional phase space; and $\varepsilon = \int \varepsilon(\vec{z})S(\vec{z})d\vec{z} / \int S(\vec{z})d\vec{z}$ is the average signal detection efficiency.

ANALYSIS OF EXPERIMENTAL DATA

After all selections, about 5.5 million events in all four configurations ((e^+, $\pi^-\pi^0$), (e^-, $\pi^+\pi^0$), (μ^+, $\pi^-\pi^0$), (μ^-, $\pi^+\pi^0$)) are selected for the fit. Figure 1 shows the distri-

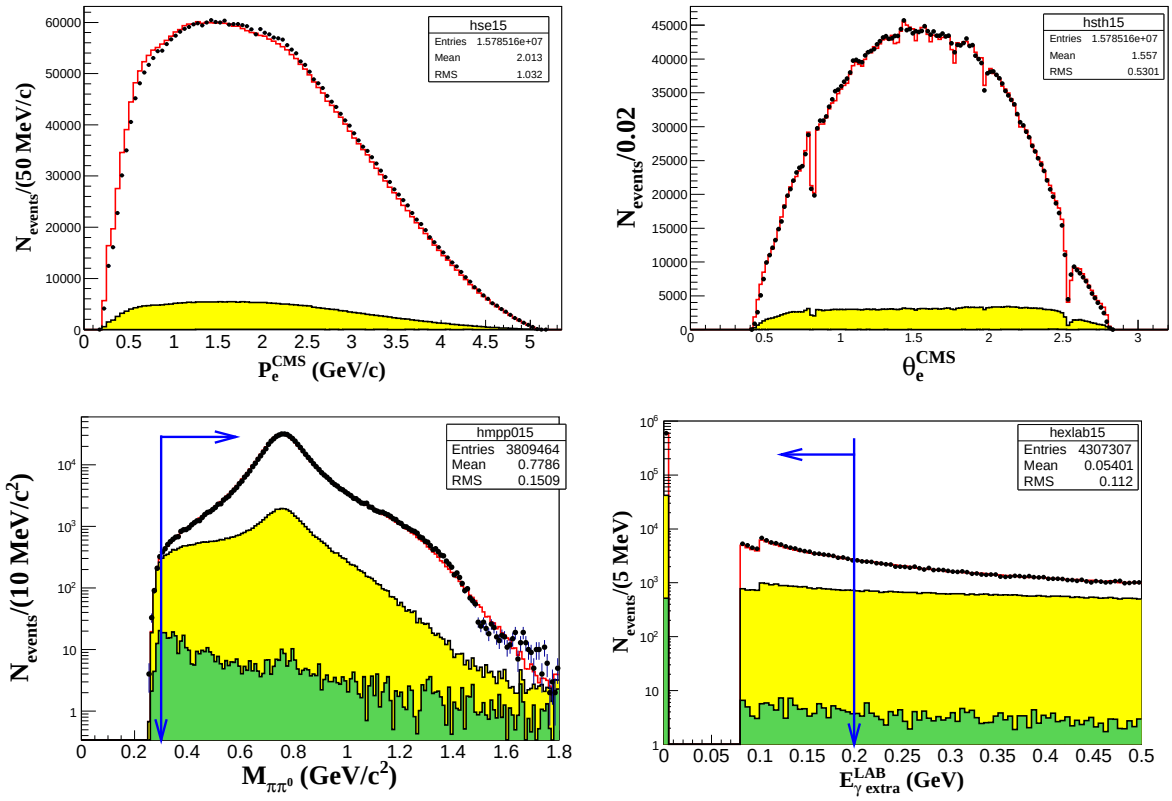

FIG. 1: Distributions of the selected (e^+, $\pi^-\pi^0$) events: e^+ momentum (upper left) and polar angle (upper right) in the c.m.s., $\pi^-\pi^0$ invariant mass (lower left), extra gamma energy in laboratory frame (lower right). Open histograms - signal MC simulation, yellow shaded histograms - the main background components from the (e^+, $\pi^-\pi^0\pi^0$) events, green shaded histograms - the remaining background, points with errors - experimental data. Blue arrows show applied selections. MC and experimental histograms are normalized to the same number of events.

butions of selected kinematical parameters for $(e^+,\ \pi^-\pi^0)$ events. Clearly, the experimental electron momentum spectrum is shifted markedly to higher momenta in comparison with the MC one. This is an artifact of the strong nonuniformity of the experimental trigger efficiency, which is not properly simulated. A special procedure has been developed to evaluate the trigger efficiency corrections, $\epsilon^{\rm TRG}_{\rm corr} = \varepsilon^{\rm TRG}_{\rm EXP}/\varepsilon^{\rm TRG}_{\rm MC}$; see Fig. 2. The trigger efficiency

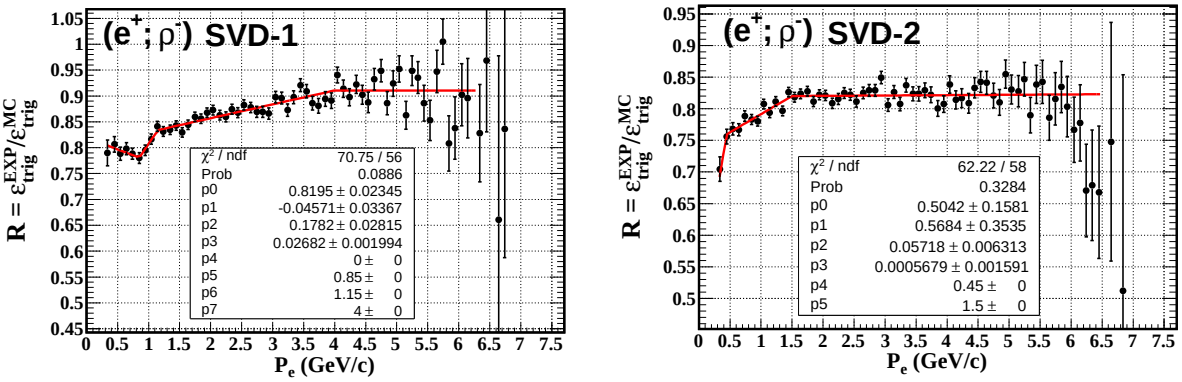

FIG. 2: Trigger efficiency correction for SVD-1 (left) and SVD-2 (right) $(e^+,\ \rho^-)$ data samples as a function of electron momentum in the laboratory frame - black points with errors. It is fitted by an empirical function shown by the red solid line.

correction as well as the lepton identification efficiency correction, $\epsilon^{\ell\rm ID}_{\rm corr}$, are incorporated in the fitter by modifying the detection efficiency in Eq. 16: $\varepsilon(\vec{z}) \to \varepsilon(\vec{z})\epsilon^{\rm TRG}_{\rm corr}(p^{\rm LAB}_\ell)\epsilon^{\ell\rm ID}_{\rm corr}(p^{\rm LAB}_\ell)$.

The result of the fit of the $(e^+,\ \rho^-)$ experimental data is illustrated in Fig. 3. Reasonable agreement can be observed for the whole energy range, although the relative difference between these spectra indicates a remaining systematic effect of about a few percent. The distribution of the likelihood per event demonstrates the acceptable quality of the fit. The distribution of the τ helicity sensitive variable ω [30] is also shown in Fig. 3. A spin-spin correlation of tau leptons is clearly demonstrated in Fig. 4 for $(e^+,\ \rho^-)$ events; the e^+ energy spectrum shape changes notably as ω varies from -1 to $+1$.

It is confirmed that the uncertainties arising from the physical and apparatus corrections to the p.d.f. are well below 1%; see Table I. The statistical uncertainties of the normalisation coefficients are kept as small as possible. The contribution to the systematic uncertainties of the Michel parameters due to the finite accuracy of the normalisation coefficients shown in Table I are evaluated with the entire available generic $\tau^+\tau^-$ MC sample; they provide the dominant contributions. We observe a correlation of about 92% between the ρ and η parameters. The slope of the corresponding error ellipse exhibits an approximate dependence of $\Delta\eta \approx 4\Delta\rho$, which is incorporated as an inflated uncertainty of the η parameter in Table I.

However, we still observe a systematic bias of the order of a few percent, especially in the $\xi_\rho\xi$ and $\xi_\rho\xi\delta$ Michel parameters. This bias originates from the remaining inaccuracies in the description of the $\ell - 3\pi$ background.

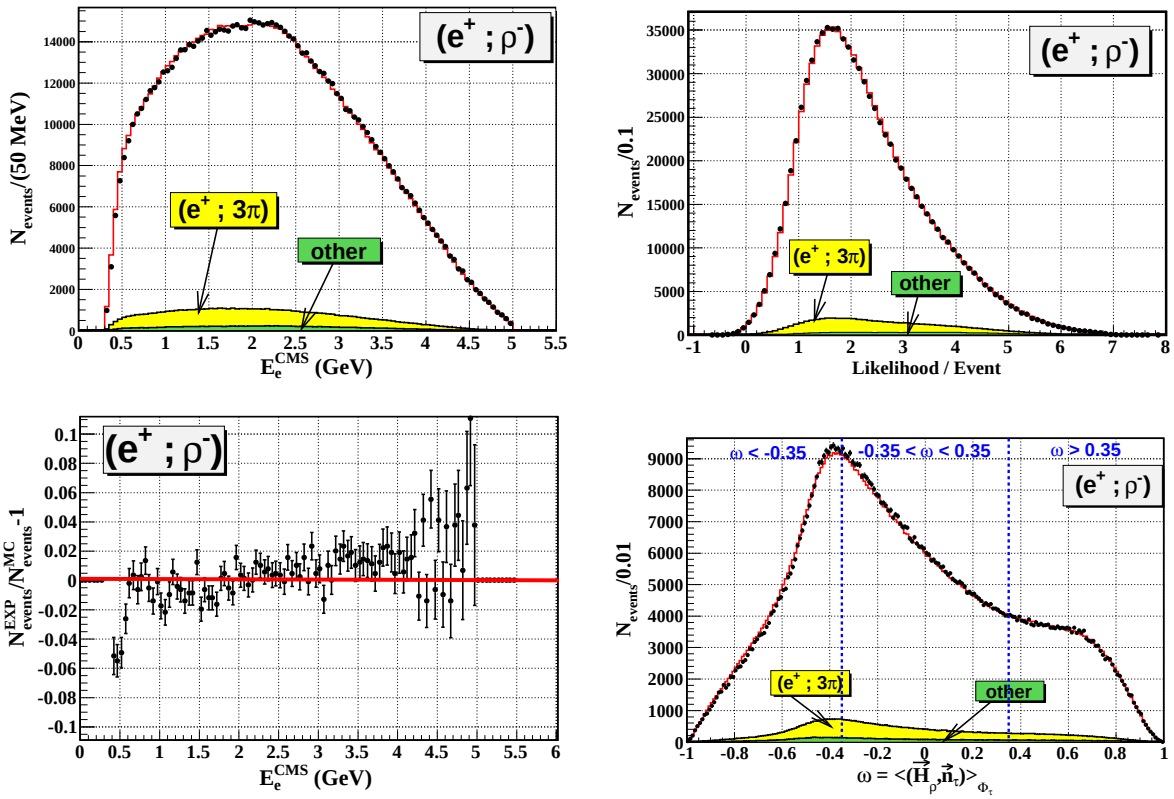

FIG. 3: Result of the fit of $(e^+,\ \rho^-)$ experimental events. e^+ energy spectrum in CMS (upper left), relative difference between experimental energy spectrum and fit result (lower left), likelihood per event (upper right) and distribution of τ helicity sensitive variable ω (lower right). Points with errors show experimental data, histogram - result of the fit. Open histograms show signal events, shaded histograms - background contributions.

SUMMARY

We present a study of Michel parameters in leptonic τ decays using a 485 fb^{-1} data sample collected at Belle. Michel parameters are extracted in the unbinned maximum likelihood fit of the $\ell - \rho$ events in the full nine-dimensional phase space. We exploit the spin-spin correlation of tau leptons to extract $\xi_\rho\xi$ and $\xi_\rho\xi\delta$ in addition to the ρ and η Michel parameters. Although systematic uncertainties coming from the physical and apparatus corrections as well as from the normalisation are below 1%, currently we still have a relatively large systematic bias in the $\xi_\rho\xi$ and $\xi_\rho\xi\delta$ parameters, which originates from the inaccurate description of the dominant $\ell - 3\pi$ background.

ACKNOWLEDGMENTS

We thank the KEKB group for the excellent operation of the accelerator; the KEK cryogenics group for the efficient operation of the solenoid; and the KEK computer group, the National Institute of Informatics, and the PNNL/EMSL computing group for valuable computing and SINET4 network support. We acknowledge support from the Ministry of

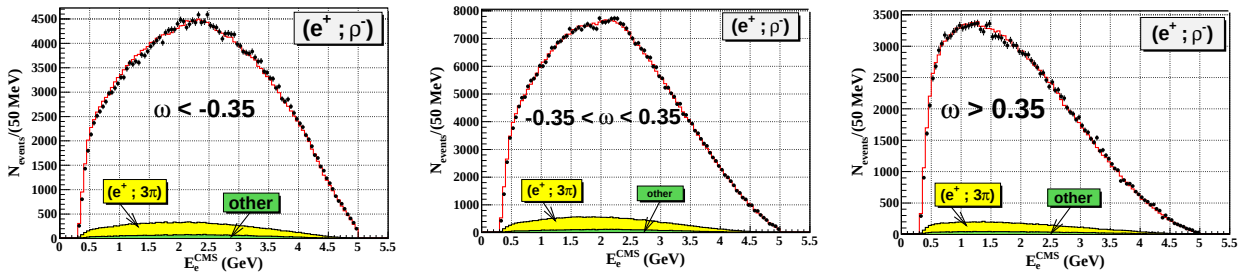

FIG. 4: Result of the fit of $(e^+,\ \rho^-)$ experimental events. Three e^+ energy spectra are shown for different ranges in ω: $\omega < -0.35$ (left), $-0.35 < \omega < 0.35$ (middle), $\omega > 0.35$ (right). Points with errors show experimental data, histogram - result of the fit. Open histograms show signal events, shaded histograms - background contributions.

TABLE I: Systematic uncertainties of Michel parameters related to physical and apparatus corrections, and accuracy of the normalisation coefficients $\mathcal{N}_i$. Values are shown in units of percent (i.e. absolute deviation of the Michel parameter is multiplied by 100%).

Source	$\sigma(\rho),\%$	$\sigma(\eta),\%$	$\sigma(\xi_\rho\xi),\%$	$\sigma(\xi_\rho\xi\delta),\%$
Physical corrections				
ISR+$\mathcal{O}(\alpha^3)$	0.10	0.30	0.20	0.15
$\tau \to \ell\nu\nu\gamma$	0.03	0.10	0.09	0.08
$\tau \to \rho\nu\gamma$	0.06	0.16	0.11	0.02
Apparatus corrections				
Resolution $\oplus$ brems.	0.10	0.33	0.11	0.19
$\sigma(E_{\rm beam})$	0.07	0.25	0.03	0.15
Normalisation				
$\Delta\mathcal{N}_1$	0.21	0.60	0.14	0.12
$\Delta\mathcal{N}_3$	< 0.01	< 0.01	0.35	0.03
$\Delta\mathcal{N}_4$	0.02	0.03	0.05	0.23
Total	0.27	0.81	0.47	0.40

Education, Culture, Sports, Science, and Technology (MEXT) of Japan, the Japan Society for the Promotion of Science (JSPS), and the Tau-Lepton Physics Research Center of Nagoya University; the Australian Research Council and the Australian Department of Industry, Innovation, Science and Research; Austrian Science Fund under Grant No. P 22742-N16 and P 26794-N20; the National Natural Science Foundation of China under Contracts No. 10575109, No. 10775142, No. 10825524, No. 10875115, No. 10935008 and No. 11175187; the Ministry of Education, Youth and Sports of the Czech Republic under Contract No. LG14034; the Carl Zeiss Foundation, the Deutsche Forschungsgemeinschaft and the VolkswagenStiftung; the Department of Science and Technology of India; the Istituto Nazionale di Fisica Nucleare of Italy; National Research Foundation of Korea Grants No. 2011-0029457, No. 2012-0008143, No. 2012R1A1A2008330, No. 2013R1A1A3007772, No. 2014R1A2A2A01005286, No. 2014R1A2A2A01002734, No. 2014R1A1A2006456; the BRL program under NRF Grant No. KRF-2011-0020333, No. KRF-2011-0021196, Center for

Korean J-PARC Users, No. NRF-2013K1A3A7A06056592; the BK21 Plus program and the GSDC of the Korea Institute of Science and Technology Information; the Polish Ministry of Science and Higher Education and the National Science Center; the Ministry of Education and Science of the Russian Federation and the Russian Federal Agency for Atomic Energy; the Slovenian Research Agency; the Basque Foundation for Science (IKERBASQUE) and the UPV/EHU under program UFI 11/55; the Swiss National Science Foundation; the National Science Council and the Ministry of Education of Taiwan; and the U.S. Department of Energy and the National Science Foundation. This work is supported by a Grant-in-Aid from MEXT for Science Research in a Priority Area ("New Development of Flavor Physics") and from JSPS for Creative Scientific Research ("Evolution of Tau-lepton Physics").

[1] W. Fetscher, H. J. Gerber and K. F. Johnson, Phys. Lett. B **173** (1986) 102.
[2] W. Fetscher and H. J. Gerber, Adv. Ser. Direct. High Energy Phys. **14** (1995) 657.
[3] K. A. Olive *et al.* (Particle Data Group), Chin. Phys. C **38** (2014) 090001.
[4] Y. -S. Tsai, Phys. Rev. D **4** (1971) 2821 [Erratum-ibid. D **13** (1976) 771].
[5] M. Fujikawa *et al.* [Belle Collaboration], Phys. Rev. D **78** (2008) 072006.
[6] W. Fetscher, Phys. Rev. D **42** (1990) 1544.
[7] K. Tamai, Nucl. Phys. B **668** (2003) 385.
[8] K. Tamai, KEK Preprint 2003-14.
[9] A. B. Arbuzov, G. V. Fedotovich, E. A. Kuraev, N. P. Merenkov, V. D. Rushai and L. Trentadue, JHEP **9710** (1997) 001 [hep-ph/9702262].
[10] A. B. Arbuzov, G. V. Fedotovich, F. V. Ignatov, E. A. Kuraev, A. L. Sibidanov, BINP Preprint 2004-70.
http://www.inp.nsk.su/activity/preprints/files/2004_070.pdf
[11] A. B. Arbuzov, G. V. Fedotovich, F. V. Ignatov, E. A. Kuraev and A. L. Sibidanov, Eur. Phys. J. C **46** (2006) 689 [hep-ph/0504233].
[12] E. A. Kuraev and V. S. Fadin, Sov. J. Nucl. Phys. **41** (1985) 466 [Yad. Fiz. **41** (1985) 733].
[13] F. A. Berends, R. Kleiss, S. Jadach and Z. Was, Acta Phys. Polon. B **14** (1983) 413.
[14] S. Jadach and Z. Was, Acta Phys. Polon. B **15** (1984) 1151 [Erratum-ibid. B **16** (1985) 483].
[15] S. Jadach and Z. Was, Comput. Phys. Commun. **36** (1985) 191.
[16] A. B. Arbuzov, Phys. Lett. B **524** (2002) 99.
[17] A. Arbuzov, A. Czarnecki and A. Gaponenko, Phys. Rev. D **65** (2002) 113006.
[18] A. Arbuzov and K. Melnikov, Phys. Rev. D **66** (2002) 093003.
[19] F. Flores-Baez *et al*, Phys. Rev. Lett. D **74** (2006) 071301(R).
[20] A. Flores-Tlalpa *et al*, Nucl. Phys. B (Proc. Suppl.) **169** (2007) 250.
[21] S. Kurokawa and E. Kikutani, Nucl. Instrum. Methods Phys. Res. Sect. A **499** (2003) 1, and other papers included in this volume; T.Abe *et al.*, Prog. Theor. Exp. Phys. **2013** (2013) 03A001 and following articles up to 03A011.
[22] Z. Natkaniec *et al.* (Belle SVD2 Group), Nucl. Instr. Meth. A **560** (2006) 1.
[23] A. Abashian *et al.* (Belle Collaboration), Nucl. Instrum. Methods Phys. Res. Sect. A **479** (2002) 117; also see detector section in J.Brodzicka *et al.*, Prog. Theor. Exp. Phys. **2012** (2012) 04D001.
[24] K. Hanagaki *et al*, Nucl. Instrum. Meth., **A485**, 490 (2002)
[25] A. Abashian *et al*, Nucl. Instr. and Meth. **A491**, 69 (2002)

[26] S. Jadach, B. F. L. Ward and Z. Was, Comput. Phys. Commun. **130** (2000) 260.
[27] Z. Was, Nucl. Phys. Proc. Suppl. **98**, 96 (2001)
[28] R. Brun *et al*, GEANT 3.21, CERN Report No. DD/EE/84-1 (1984)
[29] D. M. Schmidt, R. J. Morrison and M. S. Witherell, Nucl. Instrum. Meth. A **328** (1993) 547.
[30] M. Davier *et. al* Phys. Lett. B **306** (1993) 411.